

THE POTASSIUM-ARGON LASER EXPERIMENT (KARLE): IN SITU GEOCHRONOLOGY FOR PLANETARY ROBOTIC MISSIONS. B. A. Cohen¹, D. Devismes¹, J. S. Miller¹, and T. D. Swindle², ¹NASA Marshall Space Flight Center, Huntsville AL 35805 (Barbara.A.Cohen@nasa.gov), ²The University of Arizona, Tucson AZ 85721.

Introduction: Isotopic dating is an essential tool to establish an absolute chronology for geological events, including crystallization history, magmatic evolution, and alteration events. The capability for in situ geochronology will open up the ability for geochronology to be accomplished as part of lander or rover complement, on multiple samples rather than just those returned. An in situ geochronology package can also complement sample return missions by identifying the most interesting rocks to cache or return to Earth.

The K-Ar Laser Experiment (KArLE) brings together a novel combination of several flight-proven components to provide precise measurements of potassium (K) and argon (Ar) that will enable accurate isochron dating of planetary rocks [1]. KArLE will ablate a rock sample, measure the K in the plasma state using laser-induced breakdown spectroscopy (LIBS), measure the liberated Ar using mass spectrometry (MS), and relate the two by measuring the volume of the ablated pit by optical imaging. Our work indicates that the KArLE instrument is capable of determining the age of planetary samples with sufficient accuracy to address a wide range of geochronology problems in planetary science. Additional benefits derive from the fact that each KArLE component achieves analyses useful for most planetary surface missions.

The Potassium-Argon system: The K-Ar system is a robust choice for in situ implementation. Several ideas have been developed, to varying degrees, for in situ dating using the K-Ar system [2-4]. KArLE improves upon these by measuring K and Ar multiple times on the same sample. This decreases measurement uncertainty and increases the robustness of the interpretation. Three separate laboratories have worked over the last several years to verify the measurement capabilities and performance of this approach [1, 5-7].

KArLE measures multiple subsamples of the same rock, where each measurement provides an independent determination of K and Ar. If the Ar/K ratio is constant, a plot of K vs Ar creates a linear array with a slope proportional to the age of the rock (an isochron). Models for Martian rocks show that a 10% overall measurement uncertainty and a factor-of-two spread in K content is sufficient to achieve meaningful ages [8].

The isochron approach also obviates the need to independently assume or determine any initial or trapped contributions to ⁴⁰Ar in the sample. For example, though the younger shergottite meteorites have large uncertainties in K-Ar ages resulting from excess

Ar, Martian meteorite ages can be determined to $\pm 20\%$ using K-Ar dating [8]. A large body of knowledge from both terrestrial samples and the study of meteorites allows evaluation of loss and gain effects such as “excess Ar” or adsorption [9] and supporting data aid in the geologic interpretation of the sample.

KArLE Methodology: The LIBS-MS approach is especially promising because all of the necessary components have been flight proven and do not require further technical development for flight.

In the LIBS technique, a high-intensity (>10 MW/mm²) pulsed laser is focused on a target to ablate a small mass of material, forming a plasma, and electronically exciting constituent atoms that emit light [10, 11]. Elements in the target sample are identified by collecting, spectrally resolving, and analyzing the plasma light. Because each element’s spectrum is a unique “fingerprint,” element identification is possible, and quantitative measurements can be made based on the intensity of emission lines (e.g., [12]). The main advantage of LIBS relevant to the KArLE objectives is the absence of sample preparation; the sample can be a whole rock or chip and does not need special handling other than placement in the KArLE chamber. Coatings or dust can be ablated off without measurement.

The ChemCam LIBS is aboard the Curiosity rover, currently returning data from Mars [13]. Other LIBS instruments also are in development for planetary applications (e.g., [14] and recently-selected SuperCam). The Curiosity ChemCam instrument has demonstrated accuracy of 10% (e.g., Si of 20% to $\pm 2.0\%$) for major elements [15]. For KArLE, any LIBS instrument is suitable, requiring only a laser power density great enough to initiate plasma formation, a spectrometer with sufficient resolution (0.5 nm) to be able to separate K at 766.49 nm from Mg at 765.76 nm, and calibration to quantify K₂O concentration as low as 0.1 wt% with an uncertainty of 10% [16].

All recently-developed flight mass spectrometers, such as the Sample Analysis at Mars (SAM) QMS on Curiosity, the Ptolemy ITMS aboard the Rosetta comet investigation, and the ExoMars rover mission ITMS, have sufficient resolution (≤ 1 Da) at mass 40 to unequivocally identify ⁴⁰Ar (there are no common isobaric volatile species) and sufficient sensitivity to measure picomoles of ⁴⁰Ar and other individual species [17-19].

Because the K-Ar measurement relies on measurement of the ⁴⁰Ar liberated by laser ablation, the ablation needs to take place within an enclosed chamber.

Additionally, because Ar is a common (1-2%) atmospheric component both in terrestrial and Martian atmospheres, for Martian application, the chamber must be evacuated. For the amounts of ^{40}Ar in a typical rock released in a laser pit, the base pressure must be in the 10^{-4} Pa (10^{-6} torr) range to lower the Ar background for measurement on Mars. A miniaturized turbomolecular pump, manufactured by Creare Inc., enables the SAM instrument to achieve these pressures on Mars [18].

In the KArLE methodology, Ar is measured as the number of atoms (or moles) released from a sample, while K is measured as a fraction of the sample (weight percent). It is therefore necessary to relate the absolute MS and relative LIBS measurements to each other by determination of the mass involved in ablation. KArLE determines mass by measuring volume and density. Sample density is computed from a normative calculation based on elemental composition, or by modal mineralogy. Computed bulk density can have uncertainties of 5% even for unknown rocks [20]. Pit volume is measured using optical methods, either by z-stacking of successive images taken with a short depth of field, or by digital elevation models derived from stereo image pairs with a long depth of field. Both methods are accomplishable with currently-flying cameras such as the MER Microscopic Imager (MI), Curiosity Mars Hand Lens Imager (MAHLI), and Curiosity Remote Microimager (RMI) [21-23]. Direct sample imaging also aids in volume estimation by providing a visual estimate of porosity, which modifies the bulk density.

The performance of the individual measurements determines the precision of the KArLE experiment. Given fixed measurement uncertainties, the uncertainty in age becomes a smaller fraction of the age (more precise) as ages increase (Fig. 1a), a feature for planetary samples, which are generally older than terrestrial samples. A conservative uncertainty goal is 15% in the combined $^{40}\text{Ar}/^{40}\text{K}$ ratio ($\sigma_{\text{Ar}/\text{K}}=15\%$). Using an isochron approach further reduces uncertainty. These performance levels enable KArLE to determine the age of planetary samples 2 Ga and older to ± 100 Ma, sufficient to address a range of geochronology needs.

Extensive flight and laboratory-based work using the KArLE components establishes the limits of detection (LOD) for rocks datable by KArLE (Fig 1b). KArLE will be able to accurately date the majority of rocks encountered by Spirit, Opportunity, and Curiosity, high-K and low-K lunar rocks, and ordinary chondrites, with precision for single K-Ar analyses comparable to Martian meteorites.

KArLE Breadboard Performance: We have constructed a full breadboard of the KArLE concept. This prototype is intended to verify the measurement capa-

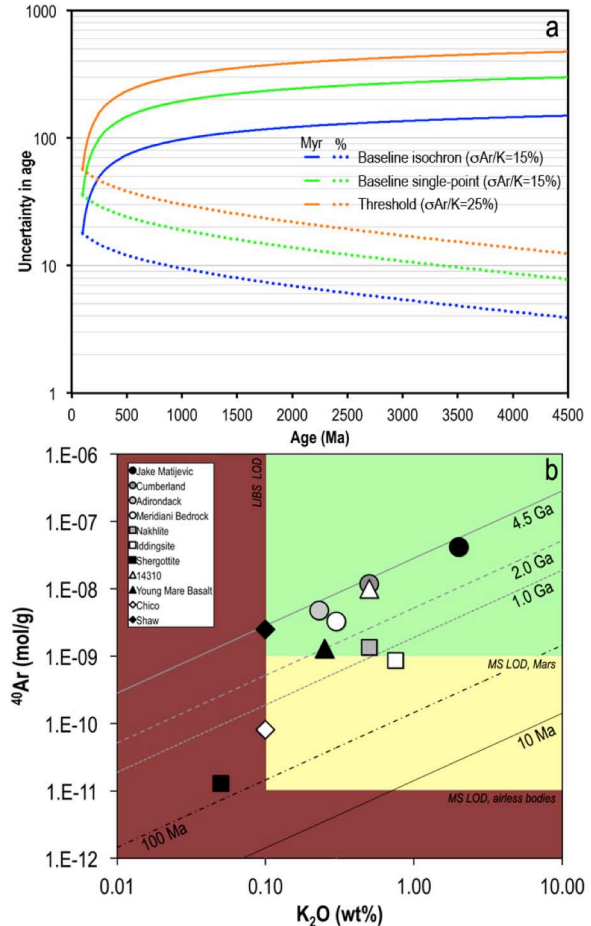


Figure 1. (a) Precision for the KArLE method as a function of age of the rock. The uncertainty in the total age is a combination of the precision of each measurement method. (b) Predicted ability of KArLE to date planetary samples from the Moon, Mars, and asteroids. The KArLE errors would be smaller than the plot symbols.

bilities and performance and to conduct trades in implementation. For this breadboard, commercial off-the-shelf parts are readily available with performance similar to flight parts [5]. We integrated an Ocean Optics LIBS 2500+ system and a Hiden 3F QMS residual gas analyzer with a test chamber, vacuum pumps, getter, and valve system. Externally, we have a Keyence VK-X100 Laser Confocal Microscope to measure the laser-generated pits. We acquired LIBS, QMS, and volume measurements on various standards to calibrate and verify the testbed instruments' performance (Fig. 2).

The relationship between the LIBS emission intensity and elemental abundance is specific to the experimental configuration and depends upon viewing geometry, depth of the ablated pit, material properties, and ambient pressure. We calibrated our LIBS K abundance curve using pressed powdered standards

with a range of K_2O content from 0.1-18 wt% K_2O and comparing the known abundance to the intensity of the K peak at 766 nm ratioed to the total integrated intensity of the spectrum. Work using LIBS in multiple laboratories have studied potential complications such as the formation of deep pits, diminished emission in vacuum, formation of a coating of melt in the pit and diffusion of volatiles, and have either shown that the effects are not large enough to cause problems or have developed strategies to mitigate them [24-26].

The Ar gas released from the sample may be measured by static mass spectrometry, such as a QMS, or dynamically, for example, in an ion-trap MS. We tested both methods. Both methods require calibration with known gas aliquots referenced to the total volume of the chamber and mass spectrometer, along with knowledge of the operating temperature. We calibrated our setup with pipettes containing both room air and pure reference gases. When referenced to calibration runs, both methods are reproducible to 2-3%.

The volume of material ablated per shot varies with material properties and optical setup (laser focus and

beam shape), but generally follows an exponentially declining trend, modified by factors related to mineral hardness and/or porosity [27], suggesting that trends in pit volume may be predicted if the relative hardness is known. More accurate and precise volumes can be measured by directly imaging the ablated pit as a set of stacked images at decreasing focal planes and using edge-detection software to create a contour map of the pit, or taking a set of stereo images that can be reconstructed into a three-dimensional digital elevation model. We tested both options in the laboratory using rover-analogous camera resolutions.

The results for all three reference pits show that stereo imaging is a suitable method for determining the volume of LIBS pits in a mission setting, readily meeting the targeted 10% uncertainty [1]. The z-stacking method is also promising, but needs a short depth of field to meet the KARLE accuracy needs ($<90 \mu m$) and further refinement in automated edge detection, which we are currently pursuing using existing software programs, to improve its precision and reproducibility.

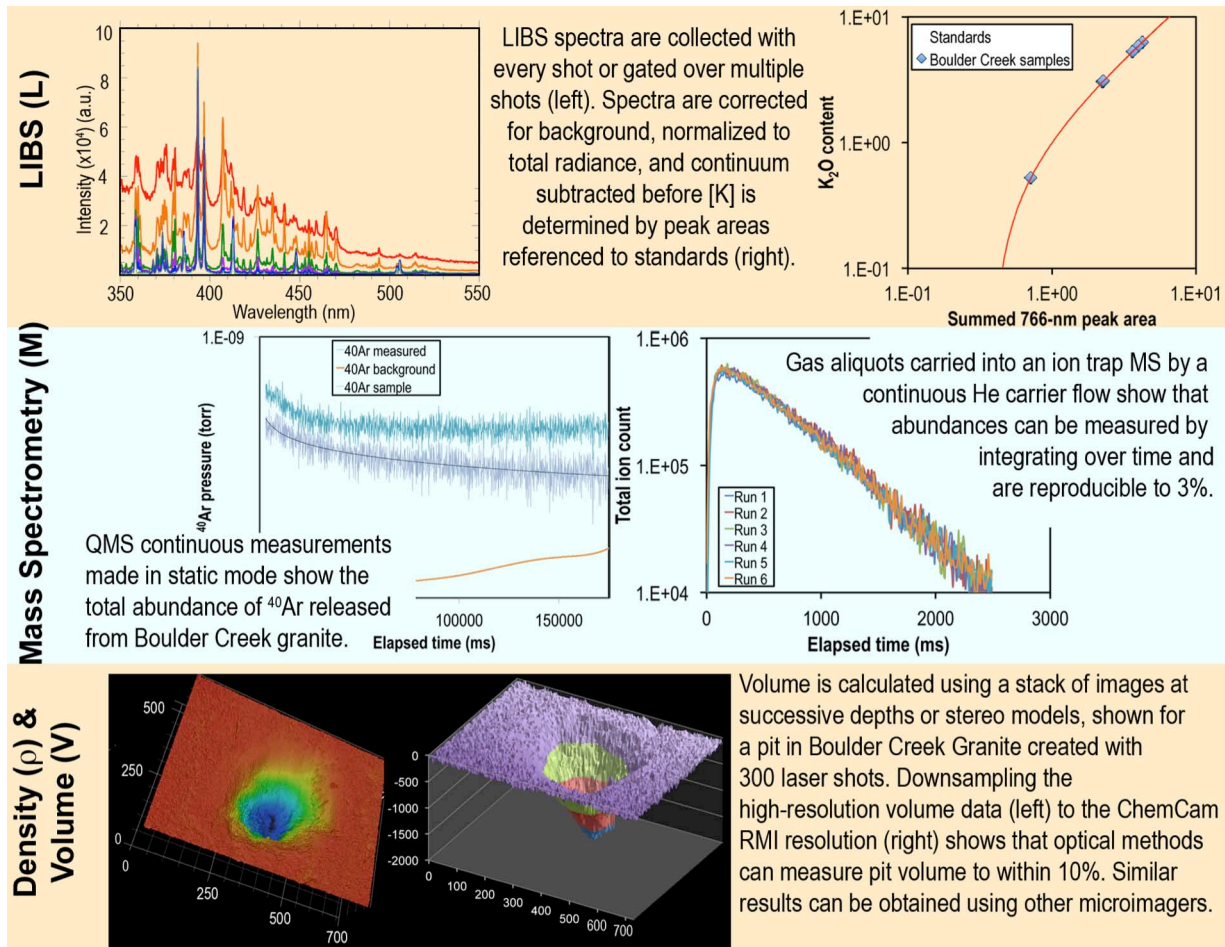


Figure 2. Example analytical results using the KARLE breadboard.

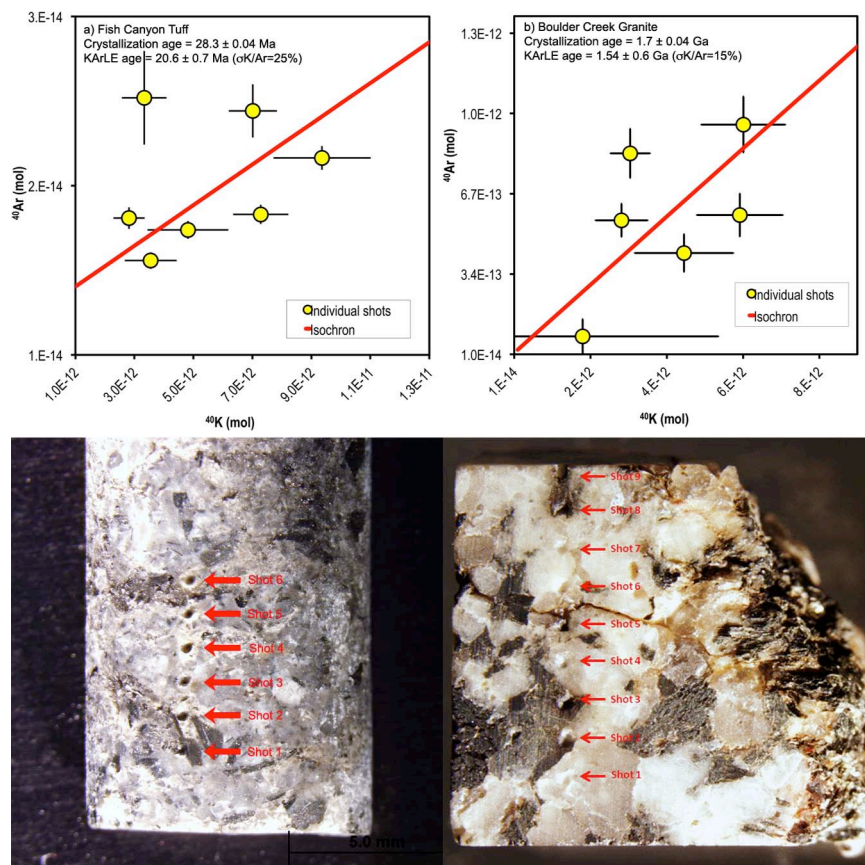


Figure 3. KARLE breadboard results for Fish Canyon Tuff (left) and Boulder Creek granite (right), along with photomicrographs of the samples after analysis. Each laser pit was created 1 mm apart without knowledge of the exposed minerals at the site. Each analysis site contained varying proportions of different minerals. Each point represents 200-500 simultaneous LIBS and MS measurements, along with pit volume measurement by laser confocal microscopy, downsampled to MAHLI resolution. Results yield whole-rock ages within error of the accepted ages. The precision depends sensitively on blanks and calibration, both of which can be substantially improved with further laboratory and flight article characterization.

Breadboard Application: We used breadboard component-level testing to demonstrate the viability of the individual KARLE analytical methods. We then conducted complete KARLE geochronologic studies of rock sample with known K-Ar age and potassium contents to demonstrate that KARLE can provide robust data with sufficiently high precision to represent major improvements in our understanding of planetary chronology. Though most meteoritic samples of known Martian origin have potassium contents only barely within the detection limits for the KARLE method, these samples do not represent the apparently higher-K rock types investigated in situ on the Martian surface (Fig. 1b). However, an appropriate analog material doesn't have to be the same age as material on the Moon or Mars – the importance lies in the ability of the techniques to measure the sample's correct age by measuring its parent and daughter with sufficient precision and accuracy, no matter its absolute age.

We selected samples of the Fish Canyon Tuff and Boulder Creek Granite for our initial studies. The Fish Canyon tuff originates in a large volcanic ash flow deposit in the San Juan volcanic field. Separated sanidine crystals are used as an interlaboratory Ar dating standard, with an age of 28.305 ± 0.036 Ma [28]. The

Boulder Creek granite forms a large batholith west of Boulder CO, composed of a gneissic quartz monzonite. It is coarser-grained than Fish Canyon and has a U-Pb age from zircons of 1714.4 ± 4.6 Ma [29]. This lithology has been previously used for other in situ geochronology tests [30]. For both samples, we computed a whole-rock density using the bulk composition for each lithology, converted to a normative composition (2.59 g/cm^3 for Fish Canyon and 2.65 g/cm^3 for Boulder Creek). Visual investigation of both samples showed very low porosity and the mineralogy did not indicate excess volatiles or alteration minerals, so the computed densities were adopted.

We collected simultaneous LIBS and QMS measurements on multiple spots on both samples by moving the sample under the laser in discrete steps and firing the laser for 300 shots each time, without attempting to confine the laser ablation to a single mineral or phase or vary the ablation parameters based on the K content. Figure 3 shows both samples after completion of the LIBS-MS runs. Each LIBS pit is 1 mm apart, approximately $300 \mu\text{m}$ in diameter and $500 \mu\text{m}$ deep, and generally comprises multiple minerals. For the LIBS measurements, spectra were collected for every laser shot, background subtracted, and the ratio of the K line

intensity to total intensity computed. The K abundance was calculated for each shot by comparing to the standard calibration, with an uncertainty introduced by the calibration curve fit line; then the average computed over all shots with an additional uncertainty of one standard deviation among shots. ^{40}Ar measurements were taken every five seconds for two minutes and extrapolated back to the inlet time to provide the abundance, with an associated uncertainty related to the line fit; followed by subtraction of a preceding blank of the same procedure. In some cases, particularly in the Boulder Creek quartz grains, the material yielded no measurable K or Ar, so were excluded from further analysis. We removed the samples to the laser confocal microscope for pit volume analysis and downsampled the data to the resolution of known microimagers.

The Fish Canyon sample yielded a best-fit isochron age of 20.6 ± 9.7 Ma, within $\sim 25\%$ of the accepted crystallization age (Fig. 3). This result is in line with the predicted uncertainty (Fig. 1a) for samples of such a young age. Our results for the Boulder Creek granite show it contains an order of magnitude more ^{40}Ar over a similar range of K content, but with markedly larger differences among individual pits due to the coarser-grained mineralogy and presence of low-K minerals. The best-fit isochron gives an age of 1.54 ± 0.6 Ga, within 10% of the accepted crystallization age.

The largest sources of uncertainty in the analysis are related to procedural blanks and the robustness of the LIBS and MS calibrations under varying conditions of the experiments. We continue to improve on these experiments in three ways: a) eliminating procedural uncertainties by better characterizing and standardizing backgrounds and blanks; b) reducing the measurement uncertainties by improving calibration with more standards and finding the optimal conditions for simultaneous measurements, and c) collecting more measurements per rock with which to construct isochrons.

Discussion: Fundamentally important scientific objectives on the Moon, Mars, and other rocky bodies can be met with in situ dating using the KArLE approach. Each component of the KArLE experiment (LIBS, MS, density, and volume) has been individually developed for application in a flight environment, yielding accurate measurements with 5-10% precision. End-to-end testing on planetary analog samples yields good results, giving ages with 25% uncertainty on very young samples ($< 50\text{Ma}$) and 10% uncertainties on older samples. These performance results predict that for planetary samples older than 2 Ga, precision will be on the order of ± 100 Ma, in line with expectations set by NASA Space Technology Roadmaps. Our component-level proof-of concept tests and our end-to-end KArLE experiments on analog samples bring the

KArLE experiment to Technology Readiness Level (TRL) 4. We plan to further develop the KArLE concept into a well-characterized flight prototype that can be tested in relevant environments.

Any geochronology instrument must be integrated into a suite of other instruments and measurements to give contextual information about the sample's location, composition, and properties to ensure that the fundamental dating assumptions are valid. Each KArLE component (LIBS, MS, camera) itself helps make these measurements. These dual-use components make KArLE an attractive way to integrate geochronology into a payload capability, on rovers or landers to Mars, the Moon, asteroids, and other rocky surfaces.

References: [1] Cohen, B. A., et al. (2014) *Geo-standards and Geoanalytical Research*, accepted. [2] Farley, K. A., et al. (2013) *GCA*, 110, 1–12. [3] Swindle, T. D., et al. (2003) *LPSC 34*, #1488. [4] Talboys, D. L., et al. (2009) *Planetary and Space Science*, 57, 1237–1245. [5] Cohen, B. A., et al. (2012) *Workshop on Planetary Instruments #1018*. [6] Cho, Y., et al. (2014) *LPSC 45*, #1205. [7] Devismes, D., et al. (2013) *EPSC2013-71*. [8] Bogard, D. D. (2009) *MAPS*, 44, 3-14. [9] Kelley, S. P. (2002) *Chemical Geology*, 188, 1–22. [10] Amoruso, S., et al. (1999) *J. Phys. B*, 32, R131 - R172. [11] Song, K., et al. (1997) *Appl. Spectrosc. Rev.*, 32, 183–235. [12] Clegg, S. M., et al. (2009) *Spectrochimica Acta B*, 64, 79–88. [13] Wiens, R. C., et al. (2013) *Spectrochimica Acta Part B*, 82, 1–27. [14] Sharma, S. K., et al. (2009) *Spectrochimica Acta Part A: Molecular and Biomolecular Spectroscopy*, 73, 468-476. [15] Williams, R. M. E., et al. (2013) *Science*, 340, 1068-1072. [16] Stipe, C. B., et al. (2012) *Spectrochimica Acta Part B: Atomic Spectroscopy*, 70, 45-50. [17] Brinckerhoff, W. B., et al. (2013) *Proceedings of the IEEE Aerospace Conference*, #2912. [18] Mahaffy, P. R., et al. (2012) *Space Sci. Rev.*, 170, 401-478. [19] Wright, I. P., et al. (2007) *Space Sci. Rev.*, 128, 363-381. [20] Fennema, A. M., et al. (2007) 1772. [21] Edgett, K. S., et al. (2012) *Space Sci. Rev.*, 170, 259-317. [22] Herkenhoff, K. E., et al. (2006) *JGR*, 111, E02S04. [23] Maurice, S., et al. (2012) *Space Sci. Rev.*, 170, 95-166. [24] Lasue, J., et al. (2012) *JGR*, 117, doi:10.1029/2011JE003898. [25] Rauschenbach, I., et al. (2010) *Spectrochim. Acta B*, 65, 758-768. [26] Sal-lé, B., et al. (2005) *Spectrochimica Acta*, 60, 479-490. [27] French, R. A., et al. (2014) *LPSC 45*, #1936. [28] Renne, P. R., et al. (2010) *GCA*, 74, 5349–5367. [29] Premo, W. R. and C. M. Fanning (2000) *Rocky Mountain Geology*, 35, 31-59. [30] Anderson, F. S., et al. (2012) *LPSC 43*, #2844.